Research Article

3-Mercaptopropyltrimethoxysilane Modified Diatomite: Preparation and Application for Voltammetric Determination of Lead (II) and Cadmium (II)

Dinh Quang Khieu,[1] Bui Hai Dang Son,[1] Vo Thi Thanh Chau,[2] Pham Dinh Du,[3] Nguyen Hai Phong,[1] and Nguyen Thi Diem Chau[4]

[1]*College of Science, Hue University, Hue City 530000, Vietnam*
[2]*Faculty of Technology, Industrial University of Ho Chi Minh City, Quang Ngai Campus, Quang Ngai City 570000, Vietnam*
[3]*Faculty of Natural Science, Thu Dau Mot University, Thu Dau Mot City 590000, Vietnam*
[4]*Department of Agriculture and Rural Development, Tam Ky City, Quang Nam Province 560000, Vietnam*

Correspondence should be addressed to Dinh Quang Khieu; dqkhieu@hueuni.edu.vn

In this study, functionalized diatomite was prepared by grafting of 3-mercaptopropyltrimethoxysilane (MPTMS) to diatomite (MPTMS-diatomite). The diatomite with thermal treatment from 100 to 700°C was functionalized by MPTMS under dry and humid conditions. The obtained MPTMS-diatomite was characterized by X-ray diffraction (XRD), thermal gravity-differential scanning calorimeter (TG-DSC), and Fourier transformation infrared (FT-IR). The results showed that an increase in treatment temperature seems to reduce the loading of MPTMS onto diatomite. The humidity of diatomite was favorable for the grafting of functional groups on the surface. The possible mechanisms of MPTMS loading to diatomite (MPTMS-diatomite) were also proposed. The performance of a carbon paste electrode (CPE) modified with MPTMS-diatomite in the simultaneous determination of Cd(II) and Pb(II) ions was addressed.

1. Introduction

Heavy metals (Hg(II), Pb(II), Cd(II), Cu(II), Co(II), Ni(II), Zn(II), etc.), which are commonly found in wastewaters discharged from chemical manufacturing, mining, extractive metallurgy, nuclear, and other industries, cause danger to humans and aquatic animals and plants and therefore must be controlled urgently [1]. The detection of heavy metal ions in water samples has received much attention over the past few years. The commonly used methods for metal analysis are atomic absorption spectrometry (AAS) and electrothermal atomic absorption spectrometry (ETAAS), inductively coupled plasma-mass spectrometry (ICP-MS), inductively coupled plasma atomic emission spectrometry (ICP-AES), and inductively coupled plasma optical emission spectrometry (ICP-OES) [2–4]. These techniques can assist quantitative analyses of the total amount of toxic metals in water samples. However, disadvantages such as instrument costs and complex operation procedures may limit the use of these techniques.

Anodic stripping voltammetry (ASV) is a useful electrochemical method for detecting trace metals because of its wide linear dynamic range and low detection limit which results from a preconcentration step performed directly in the voltammetric cell. Several porous materials have been utilized as electrode modifiers with the aim of preconcentrating the analyte at the electrode surface via a selective reaction due to special function groups grafted to electrode surface [5–10].

Diatomite, which consists of a wide variety of sized diatoms in a structure containing up to 80–90% pores, is a pale-coloured, soft, lightweight sedimentary rock composed principally of silica fossils of aquatic unicellular alga [11]. Diatomite has received considerable attention for its unique combination of physical and chemical properties including

TABLE 1: Chemical composition of diatomite (wt.%).

Elements	K	Al	Si	Ti	Fe	Others
Raw diatomite	0.34	13.07	76.02	1.31	7.68	1.58

large porosity, fine particle size, and chemical inertness [12]. Silanol groups often occur on the diatomite surface especially on the natural diatomite surface. The density of the silanol groups can be controlled by hydrating diatomite. When these silanol groups combine with organosilane through a series of chemical reaction, the functional groups at the terminal end of the organosilanes can be anchored to the surface of the diatomite to form surface activated products. The diatomite in combination with surface coated functional groups offers a potential materials for adsorption [13, 14] and modifying electrodes to determine the dye [13]. Recently, the usage of silica-based materials (especially organically modified silicates) for modifying glassy carbon electrodes (GCEs) applied to the voltammetric detection of metal ions such as Hg(II), Cd(II), and Pb(II) has been extensively reported [6, 7]. However the use of organosilane modified diatomite as an electrode modifier less pronounced so far [15]. To the best of our knowledge, the use of a 3-mercaptopropyltrimethoxysilane (MPTMS) which grafted diatomite for modifying electrode in connection with the electrochemical analysis of Pb (II) and Cd (II) has not yet been reported.

In this paper, the preparation of MPTMS modified diatomite was demonstrated. The effects of thermal treatment of diatomite and the humidity of diatomite on MPTMS functionalization and the possible proposed mechanisms of MPTMS grafting diatomite surface were discussed. The MPTMS-diatomite which was used to modify electrode for simultaneous determination of Pb(II) and Cd(II) in aqueous solution by differential pulse anodic stripping voltammetry method (DP-ASV) was also studied.

2. Experimental

2.1. Materials. Diatomite sample was collected from Phu Yen province, Vietnam, after removing organic stuff by repeated sedimentation and desiccation at 100°C. The 3-mercaptopropyltrimethoxysilane (MPTMS, >99%, Merck) and chloroform (Merck) were used as functional reagent and solvent, respectively. The chemical composition of diatomite analyzed by EDS was listed in Table 1.

All working solutions of reagents were prepared from chemicals for analysis (Merck, Germany). Acetate buffer solutions (ABS) of pH = 4,5 were prepared from CH_3COOH and CH_3COONa (Merck). pH of the ABS was adjusted by adding 1.0 M nitric acid or 1.0 M sodium hydroxide solutions into the ABS and then checking by pH meter. Working solution of Cd(II) and Pb(II) was prepared daily from stock solution (1000 ppm, Merck, Germany). Nafion ($C_7HF_{13}O_5S·C_2F_4$, Merck) was used as an adhesive and electric conductivity material.

2.2. The Functionalization of Diatomite with MPTMS (MPTMS-Diatomite). The diatomite was calcined at 100,

300, 500, and 700°C for 3 hours. The incorporation of MPTMS into calcinated diatomite was conducted under dried and humid conditions. For the dry condition, 2 grams of calcinated diatomite was mixed with 2 g of MPTMS and 36 mL of chloroform in a 250 mL flask covered with watch glass. After mixing the slurry for 4 days at ambient temperature by a magnetic stirrer, it was washed with 10 mL of chloroform and filtered through a Buchner funnel. The separated solid was dried at 70°C for 24 hours. The functionalized diatomite is denoted as 100D, 300D, 500D, and 700D. The number implies temperature at which diatomite was heat-treated prior to functionalization. For the humid condition, the calcinated diatomite was hydrated for 2 hours in a desiccator containing saturated NaCl solution at the bottom before functionalization. Two grams of hydrated diatomite was mixed with 2 g of MPTMS for two hours. The solid was filtered and the extra MPTMS was extracted with chloroform in a Soxhlet until the solution in flask was clear. The resulting samples are denoted as 100H, 300H, 500H, and 700H. With the aim of studying the applicability of the material MPTMS-diatomite, the use of MPTSE-diatomite as an electrode modifier was performed.

2.3. Voltammetric Procedure

2.3.1. Preparation of Working Electrode-Modified Electrode. The preparation procedure was carried out as [16]. In brief, glassy carbon electrode (GCE) was first polished with 0.05 μm Al_2O_3 slurries on a polishing cloth and then rinsed ultrasonically with 2 M HNO_3, absolute ethanol, and double-distilled water. Subsequently, the GCE was electrochemically cleaned by cyclic potential scan between −1.5 V and +1.5 V in 0.5 M ABS pH 4.5 with the scan rate of 0.10 V s^{-1}. After that, the electrode was rinsed with double-distilled water. Nafion-MPTMS-diatomite composite was prepared by dispersing 5.0 mg MPTMS-diatomite powder into 1.0 mL Nafion (0.1 wt%) and sonicated. The GCE was coated with 5 μL of the composite and dried at room temperature (∼25°C) (denoted as MPTMS-diatomite/GCE).

2.3.2. Voltammetric Procedure. Solution under study (final volume of 10 mL) containing 0.1 M ABS (pH 4.5) and 100 ppb Cd(II) and 200 ppb Pb(II) was transferred into the electrochemical cell with the 3 electrodes. Then, voltammetric measurement was conducted as follows:

(i) *For surveying voltammetric characteristics of Cd(II) and Pb(II) on the MPTMS-diatomite/GCE*: Cd(II) and Pb(II) was accumulated on the surface of the modified electrode at a potential of −1.2 V (E_{acc}) for an accumulated time of 60 s (t_{acc}). During this stage, the electrode was rotated at a constant rate of 1000 rpm. After that, the electrode rotation was off. Then, cyclic voltammograms were recorded from −1.2 V to +0.2 V (forward potential scan) and subsequently from +0.2 V to −1.2 V (reverse potential scan) at a scan rate of 0.1 V s^{-1}.

(ii) *For differential pulse anodic stripping voltammetric (DP-ASV) determination of Cd(II) and Pb(II) on*

electrode *MPTMS-diatomite/GCE*: during the DP-
ASV procedure, the Cd(II) and Pb(II) were accu-
mulated on the surface of the rotating modified
electrode as done for the above procedure. After that,
the electrode rotation was off for 10 s and then DP-
ASV voltammograms were recorded from −1.2 V to
+0.2 V at a scan rate of 0.02 V s^{-1} and suitable dif-
ferential voltammetry technique parameters. During
the potential anodic scan, Cd(0) and Pb(0) on the
electrode surface were oxidized to Cd(II) and Pb(II).
DP-ASV voltammograms of blank solution (without
Cd(II) and Pb(II) and prepared from double-distilled
water) were similarly recorded before each measure-
ment. The Cd(II) and Pb(II) quantitation was done by
standard addition method.

2.4. Apparatuses. The phases were monitored by powder
X-ray diffraction (XRD), recorded on 8D Advance Bucker,
Germany with CuK$_\alpha$ radiation in the range of from 20° to 60°
with a scan step size of 0.01° and a scan step time of 0.04 s. The
amounts of MPTMS incorporated into diatomite were eval-
uated by TG-DSC SETARAM under ambient atmosphere.
Morphology of diatomite was observed by scanning elec-
tron microscopy (SEM.Jeole-3432) and transmission electron
microscope (TEM) (JEOL JEM-2100F). Fourier transform
infrared (FT-IR) spectra of the typical samples (1 wt% sample
+ 99 wt% KBr) were collected on Shimadzu FT-IR 8010M; the
wavenumber range was 500–4000 cm^{-1}. A CPA-HH5 Com-
puterized Polarographic Analyzer (produced by Laboratory
of Computer Application to Chemistry, Institute of Chem-
istry, Vietnam Academy of Science and Technology) was used
for voltammetry experiments. All measurements were done
in the cell with three electrodes: a GCE with a diameter of
2.8 ± 0.1 mm used for formatting the modified electrode as
working electrode, Ag/AgCl/3 M KCl as reference electrode,
and a platinum wire as auxiliary electrode. All measurements
were carried out at room temperature.

3. Results and Discussion

*3.1. Preparation of MPTMS Modified Diatomite (MPTMS-
Diatomite).* Figure 1 shows XRD patterns of diatomite calci-
nated at 100°C, 300°C, 500°C, and 700°C. The raw diatomite
(dried at 100°C) consisted of mainly amorphous structure.
At 300°C, the characterized peak of quartz was observed
indicating that the silica in amorphous form was crystallized
to form quartz crystallites. The diffraction intensity of quartz
phase increases with an increase in calcinated temperature.
Figure 2 shows SEM and TEM observation. Morphology
of raw diatomite shows a cylindrical structure with a *ca.*
length of 10–20 μm and an internal pore diameter of about
2-3 μm. There are nearly regular arrays of submicron pore in
a diameter of *ca.* 100 nm in the wall.

In order to investigate the surface characteristics of raw
and calcined diatomite, FT-IR analyses were carried out in
the range 400–4000 cm^{-1}. The main absorption bands for
raw diatomite, as shown in Figure 3, were observed at 466,
528, 690, 798, 914, 1022, 1153, 3622, and 3695 cm^{-1}. The
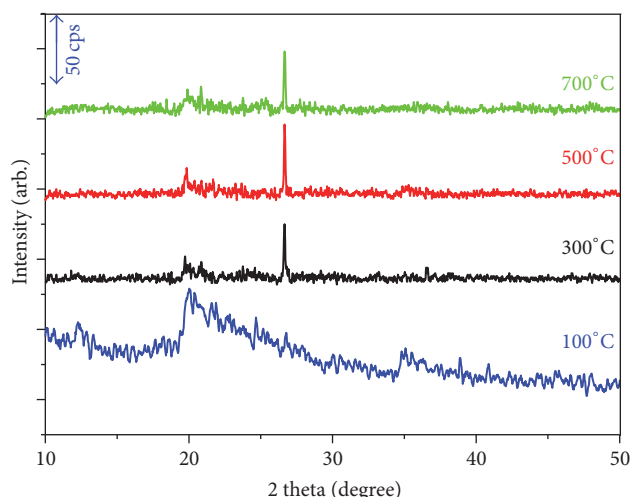absorption peaks around 466 and 528 cm^{-1} represent to the

Figure 1: XRD patterns of diatomite calcined at different tempera-
tures.

Si–O–Si bending vibration [17]. The 690 and 798 cm^{-1} bands
reflect SiO–H vibration while the 910 cm^{-1} band corresponds
to the Si–O stretching of silanol group. The bands at 1153
and 1022 cm^{-1} are strong due to stretching vibration of the
siloxane (–Si–O–Si–) groups [18]. The band at 1639 cm^{-1}
corresponds to H–O–H bending vibration of water. The
bands at 3695 and 3622 are attributed to the internal silanol
due to strongly interacting vicinal OH [19]. The surface is
also predominantly covered by physically adsorbed water in
the pore and water bounded to the surface hydroxyl groups
via H-bonds [19, 20]. By removing adsorbed water, upon
heating the diatomite at 700°C, the OH groups on diatomite
surface may be removed. The disappearance of the OH
groups may have a significant effect on MPTMS grafting to
diatomite, which is dependent on not only the pore structure
of diatomite but also the surface functional groups.

Figure 4 shows DSC and TG diagrams of diatomite
functionalized by MPTMS at dried conditions. The DSC and
TG curves were similar for all samples. The exothermic peak,
together with no any ignition loss at around 300°C, should be
attributed to the crystallization of amorphous silica to quartz.
The result also agrees with the fact that the crystallization of
quartz was detected at 300°C by XRD analysis. However, even
for sample 300D–700D which was calcinated at 300°C for
3 hours before functionalization, this peak is also observed.
This can be explained by a reconstruction to form amorphous
silica during silane treatment. The exothermic peaks and
ignition losses at around 520°C should be assigned to the
decomposition and oxidation of MPTMS incorporated into
diatomite. The hydrolysis of MPTMS into silanols occurs in
water. The silane incorporated into diatomite is due to the
condensation of silanols of diatomite and silane. In this work,
it is suggested that the silane is strongly bonded to diatomite
surface as silane is not removed by washing chloroform,
dispersed in water, or heated at 100°C. Then the amount of
MPTMS incorporated into diatomite is proportional to the
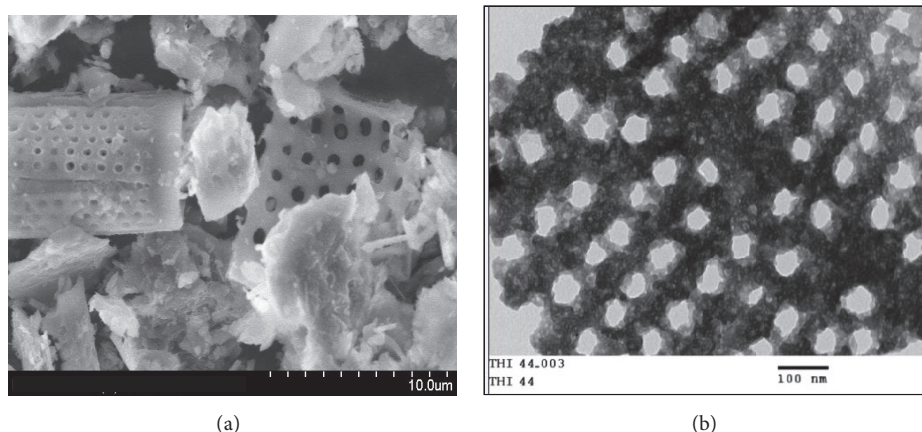amount of ignition loss in range 100°C to 700°C calculated by

(a)

(b)

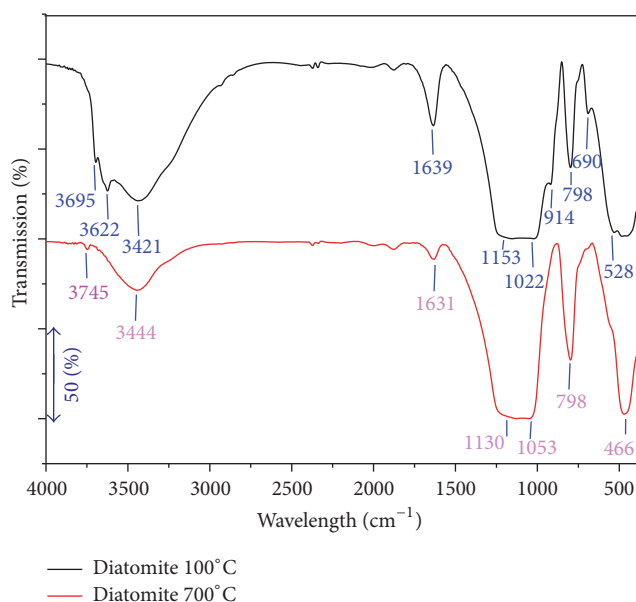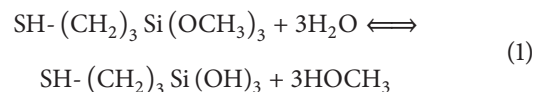FIGURE 2: (a) SEM and (b) TEM observation of raw diatomite.

FIGURE 3: Infrared spectra of (a) raw and (b) calcined diatomite at 700°C.

TG. Therefore, the ignition loss (100–700°C) was assumed as MPTMS loading to diatomite. The amount of MPTMS seems to increase slightly from 5.6% to 6.3% for D100 and D300 and decrease remarkably with a further increase in thermal treatment temperature (see Table 2).

Figure 5 shows TG-DSC diagrams of functionalized diatomite under humid conditions. The curves were similar to all samples. The thermal behaviors were also similar to the case of samples under dried conditions except for ignition loss together exothermic peaks at around 300°C observed for most cases. From Table 2, the amount of MPTMS incorporated into diatomite seems to be higher in the samples in dried conditions and the diatomite thermal treated at 100°C–300°C is most favorable for MPTMS functionalization.

There are two types of silanols, isolated and H-bonded silanols on diatomite surface [20]. At room temperature, both types of silanols are H-bonded with water. With an increase in temperature, dehydration occurs. At first, the desorption of water and the exposure of more and more isolated silanols were favorable for the silanols of silane adsorbing onto diatomite surfaces. This accounts for the fact that the high amount of MPTMS was incorporated into diatomite calcinated in the range of 100–300°C. The calcinated diatomite exposed to water-saturated medium could create more silanols, which consequently adsorb MPTMS more strongly than the diatomite under dried conditions. As the temperature increases to more than 300°C, the silanols begin to condense to form siloxane bridges that are not favorable for coupling reactions. In the case of hydrated diatomite, two decompositions of silane incorporated into diatomite are observed at around 320°C and 520°C in TG-DSC curves instead of only 520°C in the case of the dried diatomite. Based on the results reported by Johansson et al. [21] about adsorption of silane coupling agents onto kaolin surfaces, we suggest two possible mechanisms by which MPTMS react with diatomite surface. The first proposed mechanism involves four steps:

(1) MPTMS was converted to the reactive silanol formed by hydrolysis

$$
\begin{aligned}
&\text{SH-}(CH_2)_3\,Si(OCH_3)_3 + 3H_2O \Longleftrightarrow \\
&\text{SH-}(CH_2)_3\,Si(OH)_3 + 3HOCH_3
\end{aligned} \tag{1}
$$

(2) Condensation of the organosilane to oligomers is presented:

$$
(n+1)\ \text{SH-}(CH_2)_3Si(OH)_3 \longleftrightarrow HO-\underset{\underset{OH}{|}}{Si}-O-\underset{\underset{\lfloor OH \rfloor_n}{|}}{Si}-OH\ +\ n\,H_2O \tag{2}
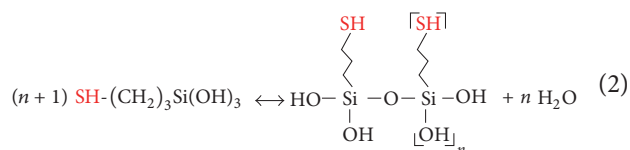$$

TABLE 2: The amount of MPTES incorporated into diatomite estimated by TG.

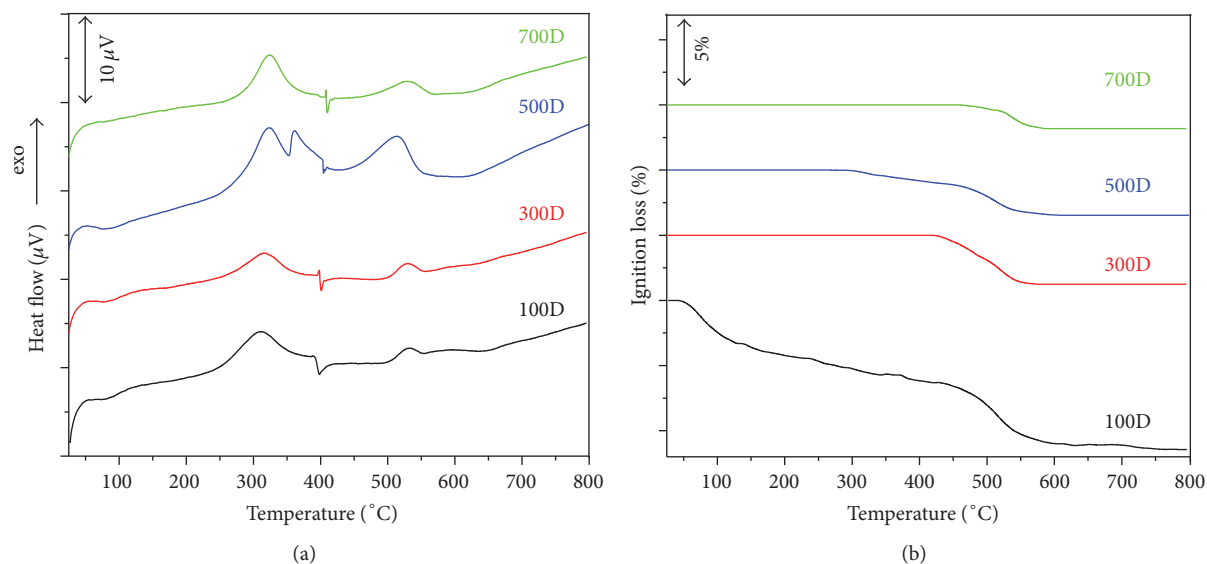|	Dried condition				Humid condition			
	100D	300D	500D	700D	100H	300H	500H	700H
Ignition loss at *ca.* 100°C (%)	5.67	0.00	0.00	0.00	3.71	2.45	0	0.00
Ignition loss at *ca.* 300°C (%)	0.00	0.00	0.00	0.00	0.00	2.02	1.31	0.80
Ignition loss at *ca.* 520°C (%)	5.44	3.76	2.55	1.82	6.99	5.69	1.70	0.97
Total ignition loss > 100°C (%)	5.44	3.76	2.55	1.82	6.99	7.71	3.01	1.77

(a)

(b)

FIGURE 4: (a) DSC diagrams; (b) TG diagrams of diatomite functionalized by MPTMS at dried condition.
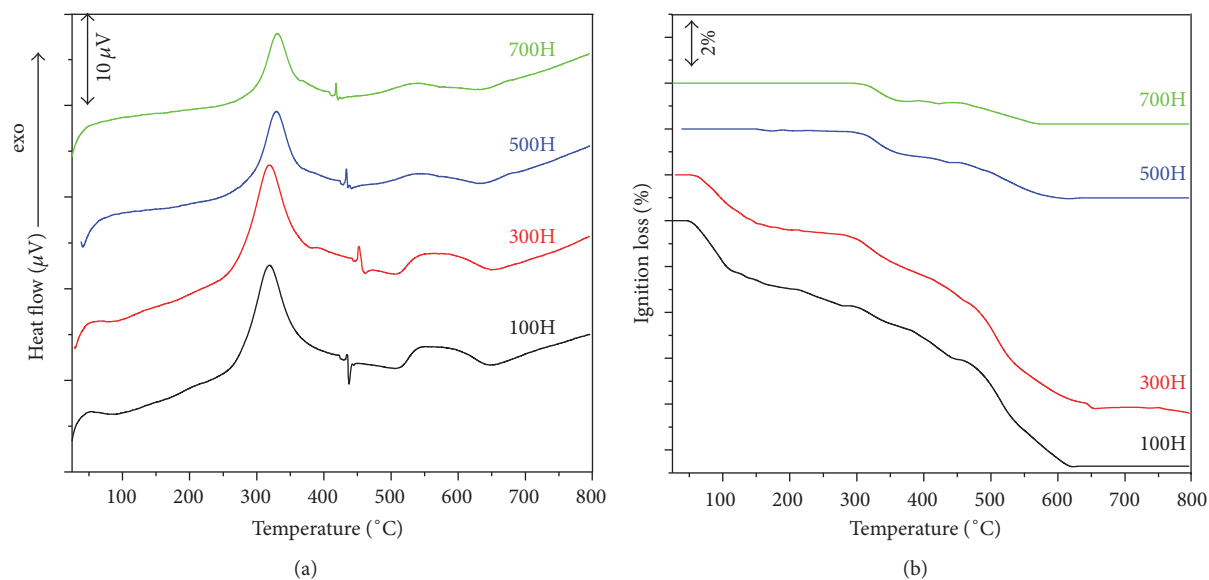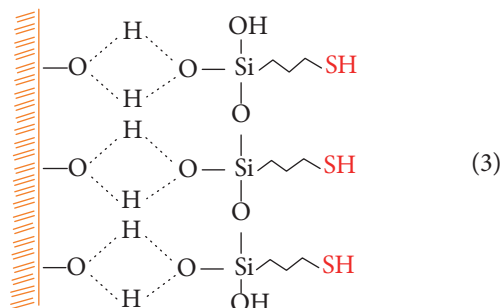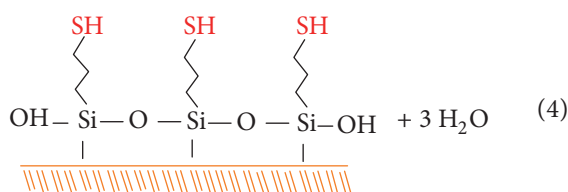

(a)

(b)

FIGURE 5: (a) DSC diagrams; (b) TG diagrams of functionalized diatomite under humid conditions.

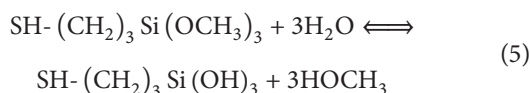(3) Formation of hydrogen bonds between the oligomers and the OH groups on the diatomite surface is presented:

$$(3)$$

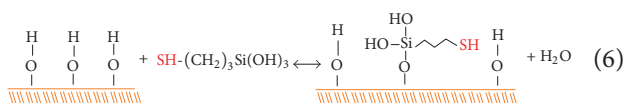(4) Finally, a covalent linkage is formed under drying

$$(4)$$

The second proposed mechanism involves only two steps:

(1) MPTMS is converted to the reactive silanol form by hydrolysis (R: CH$_2$-CH$_2$-CH$_2$-SH; X: OCH$_3$)

$$\text{SH-}(CH_2)_3\,Si\,(OCH_3)_3 + 3H_2O \rightleftharpoons$$
$$\text{SH-}(CH_2)_3\,Si\,(OH)_3 + 3HOCH_3$$

$$(5)$$

(2) The silanol groups react directly with hydroxyl groups on the diatomite surface

$$(6)$$

It is assumed that silane incorporated in diatomite by the first mechanism is more stable than one by the second mechanism. It means that it will be decomposed at higher temperature with the silane incorporated by the latter. For silane treatment with dried diatomite, the only ignition loss and exothermic peak at around 520°C could be assigned to the decomposition of silane grafting through the first mechanism. When diatomite is hydrated before silane treatment, the incorporation of MPTMS might occur through both mechanisms. Then, ignition loss and exothermic peak at around 300°C in TG-DSC for 100–700H might be assigned to decomposition of silanes in which MPTMS is grafted through the second mechanism.

The effect of hydrated times on the loading of MPTMS was also investigated. The diatomite calcined at 100°C for 3 hours was hydrated in a desiccators containing saturated NaCl solution for 0, 1, 2, 3, 6, 8, and 10 h. The functionalization was conducted as in the case of humid conditions. The

TABLE 3: The total amount of ignition loss of MPTMS-diatomite in the range 100°C–700°C.

Hydrated time	0 h	1 h	2 h	3 h	6 h	8 h	10 h
Ignition loss (%)	6.99	7.21	7.91	9.88	8.04	8.90	6.59

amount of MPTMS incorporated into diatomite estimated from TG analysis was listed in Table 3.

As can be seen, the amount of MPTMS peaked around 3 hours and then decreased as the time of hydrate was prolonged. Those results provide further evidence that water moisture favors the coupling reaction of silanols of silane and diatomite. However, the hydrated time prolonged means that there was too much water in the channel of diatomite, and the silane molecules will be significantly hydrated and condense each other instead of being bound to the wall and be removed under chloroform reflux condition; that is, the loading amount will decrease. Figure 7 shows TEM and SEM observation of MPTMS modified diatomite. The inclusions were highly dispersed on the diatomite surface (Figure 6(a)). However, pores in diatomite surface around 40–50 nm were also observed by TEM (Figure 6(b)). This means that the MPTMS-diatomite is combining highly porous structure with the binding properties of the thiol groups, leading to a high number of reactive sites that are readily accessible for the target analyte (Pb(II) and Cd(II)).

3.2. Voltammetric Characteristics of Cd(II) and Pb(II) on MPTMS-Diatomite/GCE and Limit of Detection (LOD). Figure 7 shows anodic voltammetric curves using electrodes modified by MPTMS-diatomite containing different MPTMS amounts. The percentage number in parenthesis presents the ignition loss which is assigned to as MPTMS amount. Cd(II) and Pb(II) ion showed anodic peaks at approximate -0.806 and -0.584 V in 0.1 M ABS (pH 4.5), respectively. For bare GCE and Nafion/GCE the broad oxidation peaks were observed. The intensity of anodic peak increases with an increase in MPTMS amount from 6.59% to 9.88%. A well-defined oxidation peak and high current response were observed using the MPTMS (9.88%)-diatomite electrode with highest MPTMS amount. Then, the MPTMS-diatomite with the highest amount of incorporated MPTMS was selected for modifying electrodes.

$K_3[Fe(CN)_6]/K_4[Fe(CN)_6]$ was selected as a probe to evaluate the performance of the prepared electrodes by cyclic voltammetry. Figure 8 presents the electrochemical responses of bare GCE and MPTMS-diatomite/GCE in 1.0 mM $K_3Fe(CN)_6/K_4Fe(CN)_6$ (10^{-3} M and 0.1 M KCl) solution. It is clear that the cathodic-anodic curves using electrode modified by MPTMS-diatomite were broad compared to that of bare GCE, indicating that the electron-transfer kinetics of $Fe(CN)_6^{3-}/Fe(CN)_6^{4-}$ are gradually prevented, which is probably related to the higher ohmic drop value in the electrode process [22].

The redox behavior of Cd(II) and Pb(II) was investigated by cyclic voltammetry in a potential range from -1.2 to $+0.2$ V as shown in Figure 9. The Cd(II) and Pb(II)
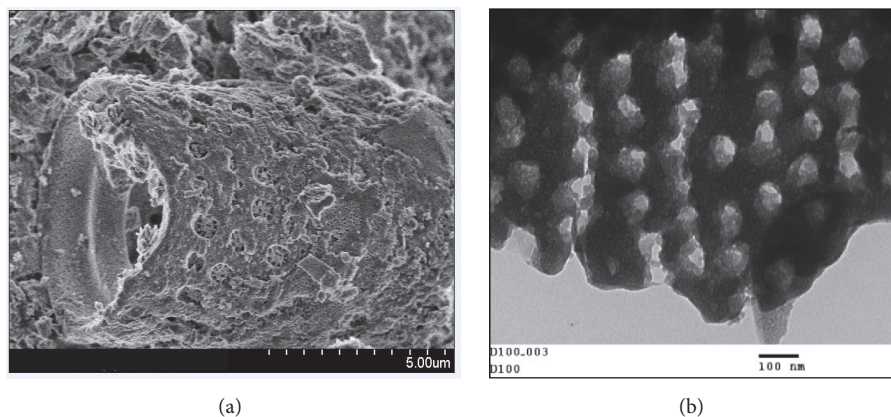
(a)

(b)

FIGURE 6: SEM (a) and (b) TEM observation of diatomite modify MPTMS.
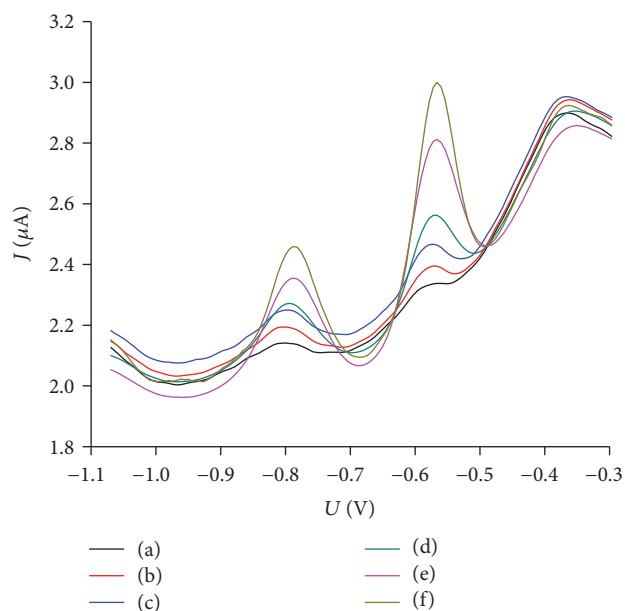

FIGURE 7: DP-ASV voltammograms for Cd(II) and Pb(II) using GCE modified by MPTMS-diatomite with differential amounts. (a) Bare GCE; (b) Nafion/GCE; (c) MPTMS (6.99%)-diatomite/GCE; (d) MPTMS (7.21%)-diatomite/GCE; (e) MPTMS (8.04%)-diatomite/GCE; (f) MPTMS (9.88%)-diatomite/GCE recorded in 0.1 M ABS (pH 4.5) containing 100 ppb Cd(II) and 200 pbb Pb(II); scan rate $0.10 \, \mathrm{V \, s^{-1}}$.

FIGURE 8: Cyclic voltammetric curves recorded in $10^{-3} \, \mathrm{M}$ $K_3[Fe(CN)_6]/K_4[Fe(CN)_6]$ solutions containing 0.1 M KCl; scan rate $0.10 \, \mathrm{V \, s^{-1}}$. (a) GCE; (b) diatomite-MPTMS/GCE.

anodic and cathodic peaks were observed for the diatomite-MPTMS/GCE; the peak separation of anodic and cathodic potentials for Cd(II) and Pb(II) were 0.226 V and 0.139 V, respectively. Therefore, the electrochemical process of Cd(II) and Pb(II) on the electrode surfaces was *quasi*-reversible. The analytical signals for electrode surface were stable for at least 5 measuring cycles with the relative standard deviation (RSD) from 2.75 to 3.5%. These results indicated very good reproducibility for Cd(II) and Pb(II) detection with the developed electrode. The anodic peak current of Cd(II) and Pb(II) (I_P) was higher than the cathodic peak current, *ca.*
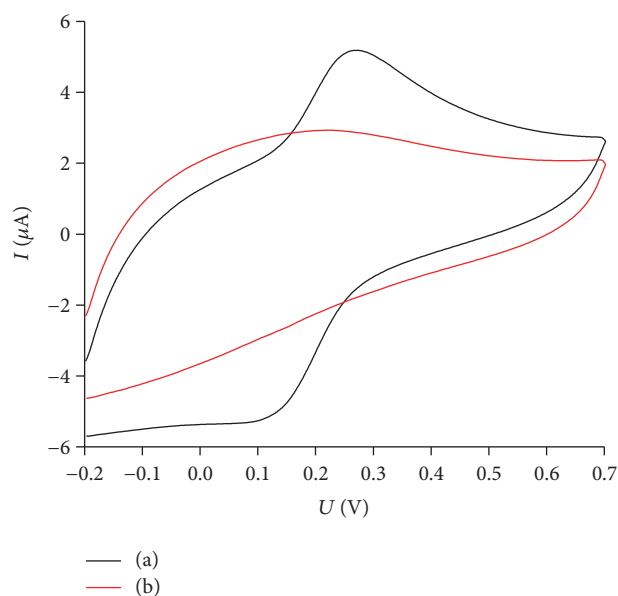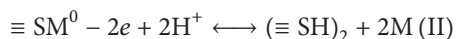
1.5-fold and 16.5-fold, respectively. It means that the anodic curves can be used for analytical signals.

The thiol group binds Cd(II) and Pb(II) to surface complexes because of its high affinity to metal ions. The metals were accumulated in electrode due to reduction reaction and then dissolved in solution through oxidation reaction. The electrochemical reaction occurred as follows [23, 24]:

$$(\equiv SH)_2 + M \, (Cd \, (II) \ \mathrm{or} \ Pb \, (II)) \longleftrightarrow \equiv SM + 2H^+$$

Complex step

$$\equiv SM + 2e \longleftrightarrow \equiv SM^0 \quad \text{Accumulation step} \tag{7}$$

$$\equiv SM^0 - 2e + 2H^+ \longleftrightarrow (\equiv SH)_2 + 2M \, (II)$$
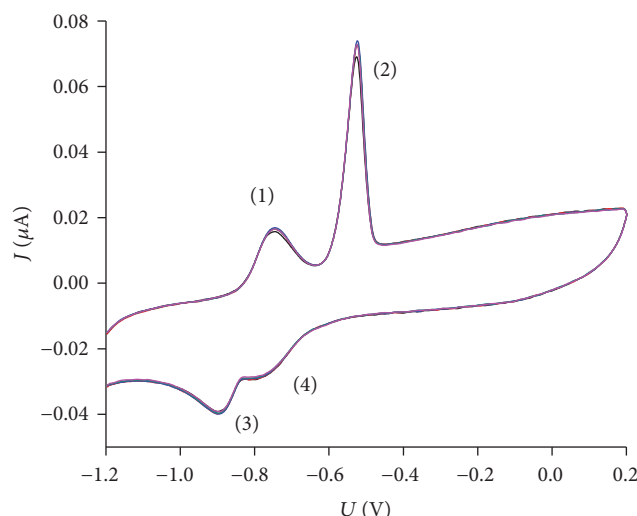
Stripping step

FIGURE 9: Cyclic voltammetric curves recorded in 0.1 M ABS (pH 4.5) containing 100 ppb Cd(II) and 200 pbb Pb(II); scan rate 0.10 V s^{-1}. (1): $I_{a,Cd}$ = 0.0152 mA, RSD = 2.75% (n = 5), and $E_{a,Cd}$ = −0.751 mV. (2): $I_{a,Pb}$ = 0.0627 mA, RSD = 2.83% (n = 5), and $E_{a,Pb}$ = −0.525 mV. (3): $I_{c,Cd}$ = 0.0102 mA, RSD = 3.50% (n = 5), and $E_{c,Cd}$ = −0.897 mV. (4): $I_{c,Pb}$ = 0.0038 mA, RSD = 2.96% (n = 5), and $E_{c,Pb}$ = −0.758 mV.
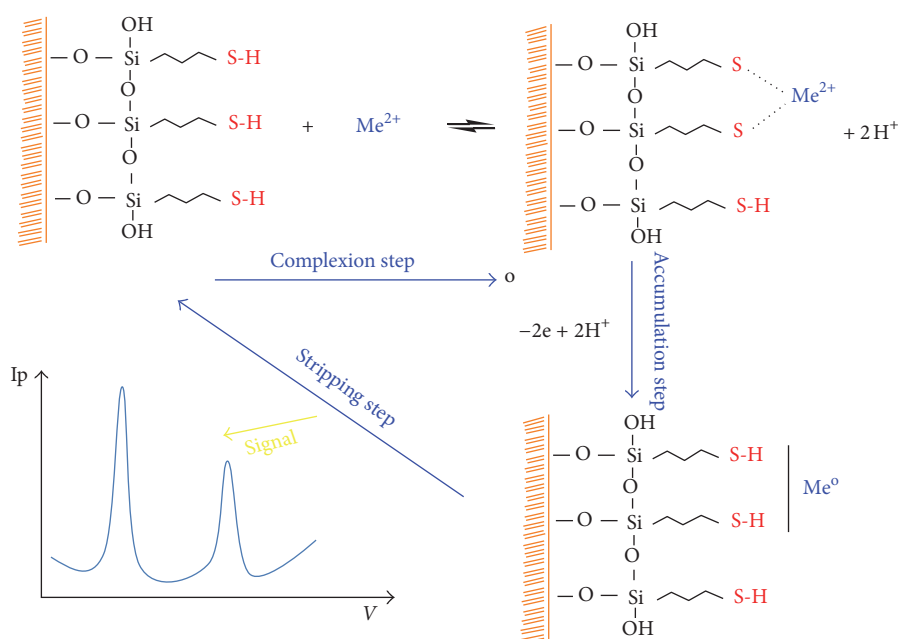

FIGURE 10: Proposed representation of preconcentration and stripping mechanism of Cd(II) and Pb(II) on MPTMS-diatomite/GCE.

Electrochemical process of Pb(II) and Cd(II) on electrodes modified by MPTMS-diatomite was illustrated by Figure 10.

Figure 11 shows the DP-ASV of Cd(II) and Pb(II) with different concentrations. An obvious anodic peaks were observed at around −0.82 and −0.61 V. These observations can be attributed to the oxidation species of Cd(II) and Pb(II), respectively, which have been deposited into the surface of MPTMS-diatomite/GCE during reduction processes. The intensity of anodic peak increased with an increase in Cd(II) and Pb(II) concentration from 20 to 300 ppb. A calibration plot of the anodic current response versus Cd(II) concentration and Pb(II) is presented in the insets of Figure 11. The results show that the current peak response was linear to the Cd(II) concentration with a R^2 of 0.999 in the range of 20–300 ppb and the Pb(II) concentration with R^2 of 0.994 in the range of 20–150 ppb. The limit of detection (LOD) was calculated on the basis of (3.3 S_a/b) criteria (S_a represents the standard deviation of the intercept while b represents the slope of the calibration curve defined for the LOD concentration range (20–300 ppb)). The LOD for Cd(II) and Pb(II) calculated was 15.9 ppb and 6.9 ppb, respectively.

Table 4 shows a comparison of MPTMS-diatomite-GCE developed with other GCEs modified with other nanoparticles for simultaneous determination of Pb(II) and Cd(II). As
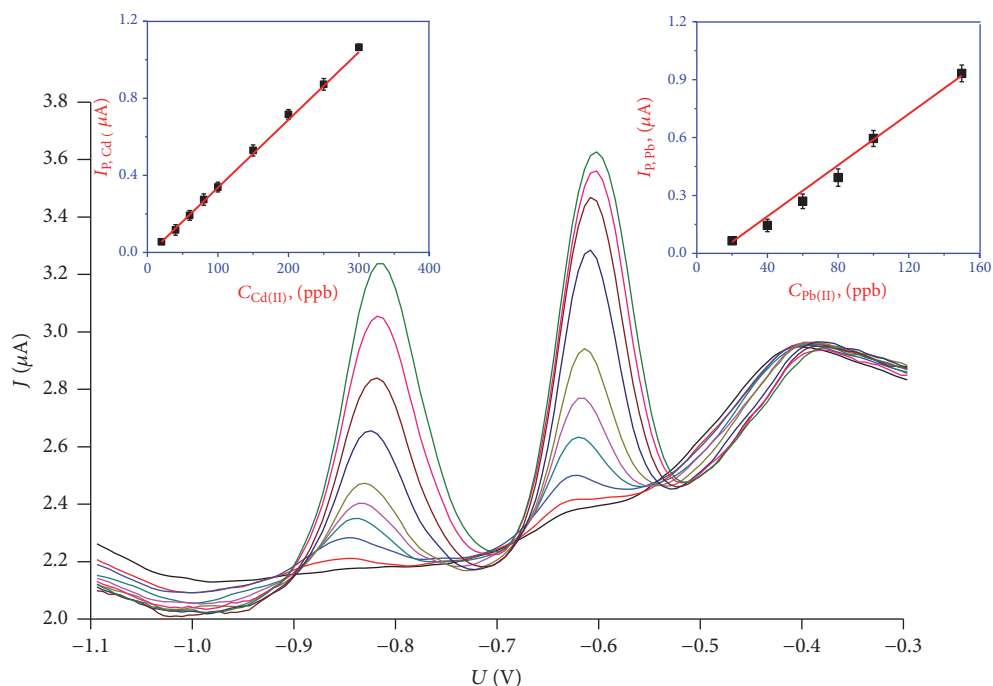
FIGURE 11: The DP-ASV voltammograms of Cd(II) and Pb(II). Conditions: the concentrations in the range of 20 to 300 ppb of the Cd(II) and Pb(II); other conditions: 0.1 M ABS (pH 4.5); $E_{acc} = -1.2$ V; $t_{acc} = 60$ s; pulse amplitude (ΔE) = 50 mV; pulse time = 40 ms; potential step = 6 mV; $\nu = 20$ mV s^{-1}; $\omega = 2000$ rpm (inset (left): a plot of stripping peak current with concentration of Cd(II); inset (right): a plot of stripping peak current with concentration of Pb(II)).

TABLE 4: Comparison of GCE modified with MPTMS-diatomite with other GCEs modified with other nanoparticles.

Electrode	Method	Linear range (ppb)	LOD (ppb)	References
MgO–Nafion/GCE	DP-ASV, ABS pH = 5.0	Cd(II): 1.1–23.6 Pb(II): 2.1–414	—	[22]
BiNPs/GCE	DP-ASV, ABS pH = 4.5	5.0–60.0	Cd(II): 0.4; Pb(II): 0.8	[25]
AuNPs/GCE	DP-ASV, ABS pH = 5.0	—	Cd(II): 20.7; Pb(II): 11.2	[26]
Padpa/Ru/GCE	DP-ASV, HCl 0,1 M	—	Cd(II): 21.7; Pb(II): 9.8	[27]
Diatomite-MPTMS/GCE	DP-ASV; ABS; pH = 4.5	Cd(II): 20–300 Pb(II): 20–150	Cd(II): 15.9; Pb(II): 6.9	This work

Glassy carbon electrode (GCE); bismuth nanoparticles (BiNPs); gold nanoparticles (AuNPs); tris(2,2′-bipyridyl)Ru(II) (Padpa/Ru).

seen in Table 4, the GCE modified with MPTMS-diatomite developed in the present work shows good LOD compared with other similar materials/GCE reported previously in the literature [21–24]. This indicates that MPTMS-diatomite is a potential material for electrode modifiers.

4. Conclusions

The effects of functionalization conditions on the loading of MPTMS in diatomite were investigated. Diatomite from Phu Yen consists of mainly amorphous structure. The crystallization to form quartz occurs at more than 300˚C. The diatomite with thermal treatment in the range of 100–300˚C is favorable for functionalization. The humidity of diatomite also affects the functionalization level significantly. The MPTMS loading around 9.8% peaked as diatomite was hydrated for 3 hours.

We have demonstrated that MPTMS-diatomite is useful to prepare chemically modified glassy carbon electrodes. The electrode modified by MPTMS-diatomite exhibited potential for the use of the simultaneous determination of cadmium and lead by DP-ASV. The stripping peak currents of the two metal ions had linear relationships with the concentrations in the range of 20 to 300 ppb (i (μA) = $-0.0202 + 0.0036$ C (ppb), $R^2 = 0.9997$) for Cd(II) and 20 to 150 ppb (i (μA) = $-0.1179 + 0.0069$ C (ppb), $R^2 = 0.9943$) for Pb(II). The LOD for Cd(II) and Pb(II) calculated was 15.9 ppb and 6.9 ppb.

Conflicts of Interest

The authors declare that there are no conflicts of interest regarding the publication of this paper.

References

[1] L. Cui, Y. Wang, L. Gao et al., "EDTA functionalized magnetic graphene oxide for removal of Pb(II), Hg(II) and Cu(II) in water treatment: adsorption mechanism and separation property," *Chemical Engineering Journal*, vol. 281, pp. 1–10, 2015.

[2] F. A. Aydin and M. Soylak, "Separation, preconcentration and inductively coupled plasma-mass spectrometric (ICP-MS) determination of thorium(IV), titanium(IV), iron(III), lead(II) and chromium(III) on 2-nitroso-1-naphthol impregnated MCI GEL CHP20P resin," *Journal of Hazardous Materials*, vol. 173, no. 1-3, pp. 669–674, 2010.

[3] J. Otero-Romaní, A. Moreda-Piñeiro, P. Bermejo-Barrera, and A. Martin-Esteban, "Inductively coupled plasma-optical emission spectrometry/mass spectrometry for the determination of Cu, Ni, Pb and Zn in seawater after ionic imprinted polymer based solid phase extraction," *Talanta*, vol. 79, no. 3, pp. 723–729, 2009.

[4] K. Ndung'u, S. Hibdon, and A. R. Flegal, "Determination of lead in vinegar by ICP-MS and GFAAS: evaluation of different sample preparation procedures," *Talanta*, vol. 64, no. 1, pp. 258–263, 2004.

[5] A. Maghear, M. Etienne, M. Tertiş, R. Sandulescu, and A. Walcarius, "Clay-mesoporous silica composite films generated by electro-assisted self-assembly," *Electrochimica Acta*, vol. 112, pp. 333–341, 2013.

[6] M. M. Abdel-Galeil, M. M. Ghoneim, H. S. El-Desoky, T. Hattori, and A. Matsuda, "Anodic stripping voltammetry determination of lead ions using highly sensitive modified electrodes based on multi-walled carbon nanotube," *Journal of Chemistry and Biochemistry*, vol. 2, no. 2, 2014.

[7] P. Zhang, S. Dong, G. Gu, and T. Huang, "Simultaneous determination of Cd^{2+}, Pb^{2+}, Cu^{2+} and Hg^{2+} at a carbon paste electrode modified with ionic liquid-functionalized ordered mesoporous silica," *Bulletin of the Korean Chemical Society*, vol. 31, no. 10, pp. 2949–2954, 2010.

[8] A. Sánchez, S. Morante-Zarcero, D. Pérez-Quintanilla, I. Sierra, and I. Del Hierro, "Determination of Hg(II) in natural waters using a carbon paste electrode modified with hybrid mesostructured silica nanoparticles," *Sensors and Actuators, B: Chemical*, vol. 163, no. 1, pp. 38–43, 2012.

[9] P. Kula, Z. Navrátilová, P. Kulová, and M. Kotoucek, "Sorption and determination of Hg(II) on clay modified carbon paste electrodes," *Analytica Chimica Acta*, vol. 385, no. 1-3, pp. 91–101, 1999.

[10] Z. Navrátilová and P. Kula, "Clay modified electrodes: present applications and prospects," *Electroanalysis*, vol. 15, no. 10, pp. 837–846, 2003.

[11] Y. Al-Degs, M. A. M. Khraisheh, and M. F. Tutunji, "Sorption of lead ions on diatomite and manganese oxides modified diatomite," *Water Research*, vol. 35, no. 15, pp. 3724–3728, 2001.

[12] M. A. Al-Ghouti, M. A. M. Khraisheh, S. J. Allen, and M. N. Ahmad, "The removal of dyes from textile wastewater: a study of the physical characteristics and adsorption mechanisms of diatomaceous earth," *Journal of Environmental Management*, vol. 69, no. 3, pp. 229–238, 2003.

[13] J. Zhang, T. Ding, Z. Zhang, L. Xu, and C. Zhang, "Enhanced adsorption of trivalent arsenic from water by functionalized diatom silica shells," *PLoS ONE*, vol. 10, no. 4, Article ID e0123395, 2015.

[14] Y. Yu, J. Addai-Mensah, and D. Losic, "Functionalized diatom silica microparticles for removal of mercury ions," *Science and Technology of Advanced Materials*, vol. 13, no. 1, Article ID 015008, 2012.

[15] I. K. Tonlé, E. Ngameni, H. L. Tcheumi, V. Tchiéda, C. Carteret, and A. Walcarius, "Sorption of methylene blue on an organoclay bearing thiol groups and application to electrochemical sensing of the dye," *Talanta*, vol. 74, no. 4, pp. 489–497, 2008.

[16] T. Zhang, L. Zeng, L. Han et al., "Ultrasensitive electrochemical sensor for p-nitrophenyl organophosphates based on ordered mesoporous carbons at low potential without deoxygenization," *Analytica Chimica Acta*, vol. 822, pp. 23–29, 2014.

[17] G. Rytwo, D. Tropp, and C. Serban, "Adsorption of diquat, paraquat and methyl green on sepiolite: experimental results and model calculations," *Applied Clay Science*, vol. 20, no. 6, pp. 273–282, 2002.

[18] R. A. Shawabkeh and M. F. Tutunji, "Experimental study and modeling of basic dye sorption by diatomaceous clay," *Applied Clay Science*, vol. 24, no. 1-2, pp. 111–120, 2003.

[19] M. A. M. Khraisheh, M. A. Al-Ghouti, S. J. Allen, and M. N. Ahmad, "Effect of OH and silanol groups in the removal of dyes from aqueous solution using diatomite," *Water Research*, vol. 39, no. 5, pp. 922–932, 2005.

[20] P. Yuan, D. Q. Wu, H. P. He, and Z. Y. Lin, "The hydroxyl species and acid sites on diatomite surface: a combined IR and Raman study," *Applied Surface Science*, vol. 227, no. 1–4, pp. 30–39, 2004.

[21] U. Johansson, A. Holmgren, W. Forsling, and R. L. Frost, "Adsorption of silane coupling agents onto kaolinite surfaces," *Clay Minerals*, vol. 34, no. 2, pp. 239–246, 1999.

[22] Z. Wu, C. Xu, H. Chen et al., "Mesoporous MgO nanosheets: 1,6-hexanediamin-assisted synthesis and their applications on electrochemical detection of toxic metal ions," *Journal of Physics and Chemistry of Solids*, vol. 74, no. 7, pp. 1032–1038, 2013.

[23] C. Hu, K. Wu, X. Dai, and S. Hu, "Simultaneous determination of lead(II) and cadmium(II) at a diacetyldioxime modified carbon paste electrode by differential pulse stripping voltammetry," *Talanta*, vol. 60, no. 1, pp. 17–24, 2003.

[24] S. Ramezani, M. Ghobadi, and B. N. Bideh, "Voltammetric monitoring of Cd (II) by nano-TiO_2 modified carbon paste electrode sensitized using 1,2-bis-[o-aminophenyl thio] ethane as a new ion receptor," *Sensors and Actuators, B: Chemical*, vol. 192, pp. 648–657, 2014.

[25] D. Yang, L. Wang, Z. Chen, M. Megharaj, and R. Naidu, "Anodic stripping voltammetric determination of traces of Pb(II) and Cd(II) using a glassy carbon electrode modified with bismuth nanoparticles," *Microchimica Acta*, vol. 181, no. 11-12, pp. 1199–1206, 2014.

[26] X. Xu, G. Duan, Y. Li et al., "Fabrication of gold nanoparticles by laser ablation in liquid and their application for simultaneous electrochemical detection of Cd^{2+}, Pb^{2+}, Cu^{2+}, Hg^{2+}," *ACS Applied Materials and Interfaces*, vol. 6, no. 1, pp. 65–71, 2014.

[27] E. A. Khudaish, M. M. Al-Hinaai, and S. H. Al-Harthi, "A solid-state sensor based on tris(2,2′-bipyridyl)ruthenium(II)/poly(4-aminodiphenylamine) modified electrode: characterization and applications," *Sensors and Actuators, B: Chemical*, vol. 185, pp. 478–487, 2013.